United States
Department of
Agriculture

**Natural
Resources
Conservation
Service**

**Part 654 Stream Restoration Design
National Engineering Handbook**

Chapter 12 Channel Alignment and Variability Design

Issued August 2007

Cover photo: Where alteration of a stream or channel is needed, planform may be modified to achieve the designed flow velocities by changing the channel length, as well as the gradient.

Advisory Note

Techniques and approaches contained in this handbook are not all-inclusive, nor universally applicable. Designing stream restorations requires appropriate training and experience, especially to identify conditions where various approaches, tools, and techniques are most applicable, as well as their limitations for design. Note also that product names are included only to show type and availability and do not constitute endorsement for their specific use.

Chapter 12 Channel Alignment and Variability Design

Contents

Tables

Figures

Chapter 12 Channel Alignment and Variability Design

654.1200 Purpose

Natural channel design includes establishment of a stable planform and often the incorporation of variability within the channel. The designer of a channel is also often asked to provide an assessment of natural bankline migration, as well. The purpose of this chapter is to provide systematic hydraulic design methodologies that can be used in the performance of these tasks. A wide variety of sources and techniques are available to the designer to make these assessments. This chapter provides overviews, descriptions, and examples illustrating some of the most common design techniques.

654.1201 Introduction

Natural channels are rarely perfectly linear and straight. While there are exceptions, and while boundary constraints may require a straight constructed channel, most natural channels exhibit at least some degree of sinuosity in their planform. Therefore, the assessment and design of a stable channel planform is an important part of any open channel design.

Planform design parameters include the meander wavelength, radius of curvature, sinuosity, and general alignment. Several of these variables are illustrated in figure 12–1 (Federal Interagency Stream Restoration Working Group (FISRWG) 1998). Several techniques that can be used to approximate natural channel alignments are presented in this chapter.

Natural channels rarely exhibit a uniform cross section. In fact, the variability often provides important ecological benefits. Since variability in a channel section is expected in natural channels, the designer of a natural channel restoration project is often asked to incorporate similar variability into the design. Generalized morphologic relationships for channel variability in streams and rivers are described in this chapter. Material from regionally specific studies is presented for illustration.

Figure 12–1 Variables used to describe channel alignment and planform

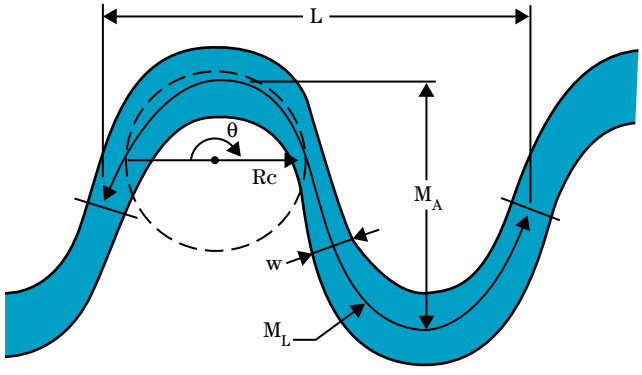

L Meander wavelength
M_L Meander arc length
w Average width at bankfull discharge
M_A Meander amplitude
Rc Radius of curvature
θ Arc angle

654.1202 Planform

This step in the design process involves laying out a planform after determining a meander wavelength and an appropriate channel length for one meander wavelength. Channel sinuosity is defined as the channel centerline length divided by the length of the valley centerline. It is determined from the calculated channel slope and valley slope. Analogy, hydraulic geometry, and analytical methods are employed to determine both the meander wavelength and a planform.

To apply the analogy method, a reference or control reach is located on either the study stream or another suitable stream. From this reach, a template for the meander planform is developed. This may be problematic due to the nonavailability of a suitable reference reach or subtle, but important fluvial, sedimentary, or morphological differences between a reference reach and the study reach.

Alternatively, meander wavelength can be determined using hydraulic geometry techniques. The most reliable hydraulic geometry relationship is wavelength versus width. As with the determination of channel width, preference is given to wavelength predictors from stable reaches of the existing stream either in the project reach or in reference reaches. The channel trace may also be determined analytically using the sine-generated curve. Finally, a string cut to the appropriate length can be laid on a map and fit to existing constraints and to the proper wavelength to form a meandering planform.

When uncertain about the appropriate technique, many practitioners use both analogy and hydraulic geometry and look for points of convergence in the recommendations. It is also important to note that planform flexibility may be limited by riparian features, infrastructure, land use, or other restrictions on the right-of-way. These factors may preclude the use of meanders with the amplitudes suggested from the described analogy or hydraulic geometry methods.

Braided channel systems are an important exception to much of the material presented in this chapter. Braided stream systems can exist naturally in estuarine, lacustrine, and glacial landscapes and valleys. These systems have depositional requirements and physical characteristics that are very different from single-thread channels. For braided streams, a single or dual thread channel reconstruction may be inappropriate and carry a potentially high risk of failure.

(a) Hydraulic geometry for meander wavelength

A composite relationship has been developed by Thorne and Soar (2001), combining 9 data sets and 438 sites. Their mean linear regression predictor for wavelength is:

$$\lambda = 10.23W \qquad \text{(eq. 12–1)}$$

where:

λ = meander wavelength
W = channel width in any consistent units of measurement

Definitions of planform descriptive variables are shown in figure 12–2. Confidence bands about this equation are shown in figure 12–3. The r^2 for the

Figure 12–2 Planform descriptive variables

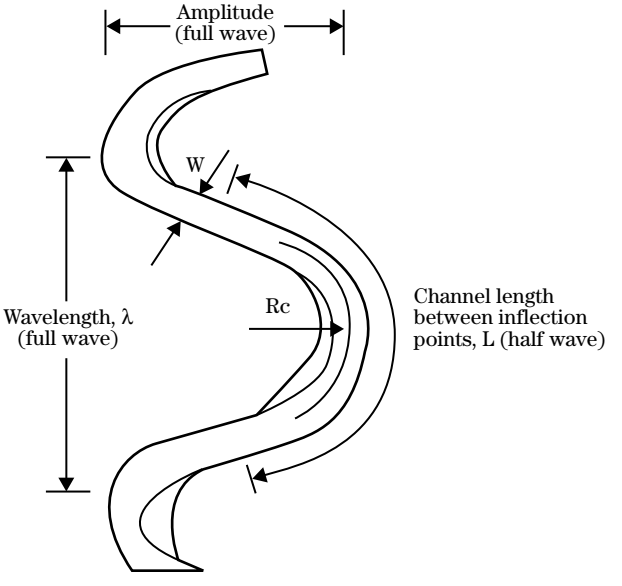

wavelength equation was 0.88 for a linear regression equation, with a variable exponent on W. This exponent was found not to be significantly different from 1.0, so the exponent was fixed at 1.0 for convenience. Only sites with sinuosities of at least 1.2 and bankfull widths between 1 meter and 1,000 meters were used in development of this regression equation. Within these constraints, meander wavelengths range between 10.4 meters and 19,368 meters, and sinuosity values range between 1.2 and 5.3. The equation, corrected for bias, is:

$$\lambda = 11.85W \qquad \text{(eq. 12–2)}$$

An unbiased hydrologic equation for meander wavelength suitable for engineering design, within 95 percent confidence limits on the mean response is:

$$\lambda = (11.26 \text{ to } 12.47)W \qquad \text{(eq. 12–3)}$$

According to Hey (1976) and Thorne (1997), twice the distance between successive riffles (or pools) in a straight channel should equal $4\pi W$, or $12.57W$. This is based on the assumption that the average size of the largest macroturbulent eddies (or helical flow cell) is half the channel width. Equation 12–3 shows that the upper range of stable meander wavelengths is numerically very close to this value and similar to the coefficient of 12.34 given by Richards (1982). This corroborates the assertion by Leopold and Wolman (1957, 1960) that the matching of waveforms in bed topography and planform is related to the mechanics of the flow and, in particular, to the turbulent flow structures responsible for shaping the forms and features of meandering channels.

Table 12–1 shows the data sources (438 sites) used in the development of these equations.

Figure 12–3 Hydraulic geometry relationship for meander wavelength with confidence intervals, λ = 10.23W, based on a composite data set of 438 sites in a variety of areas

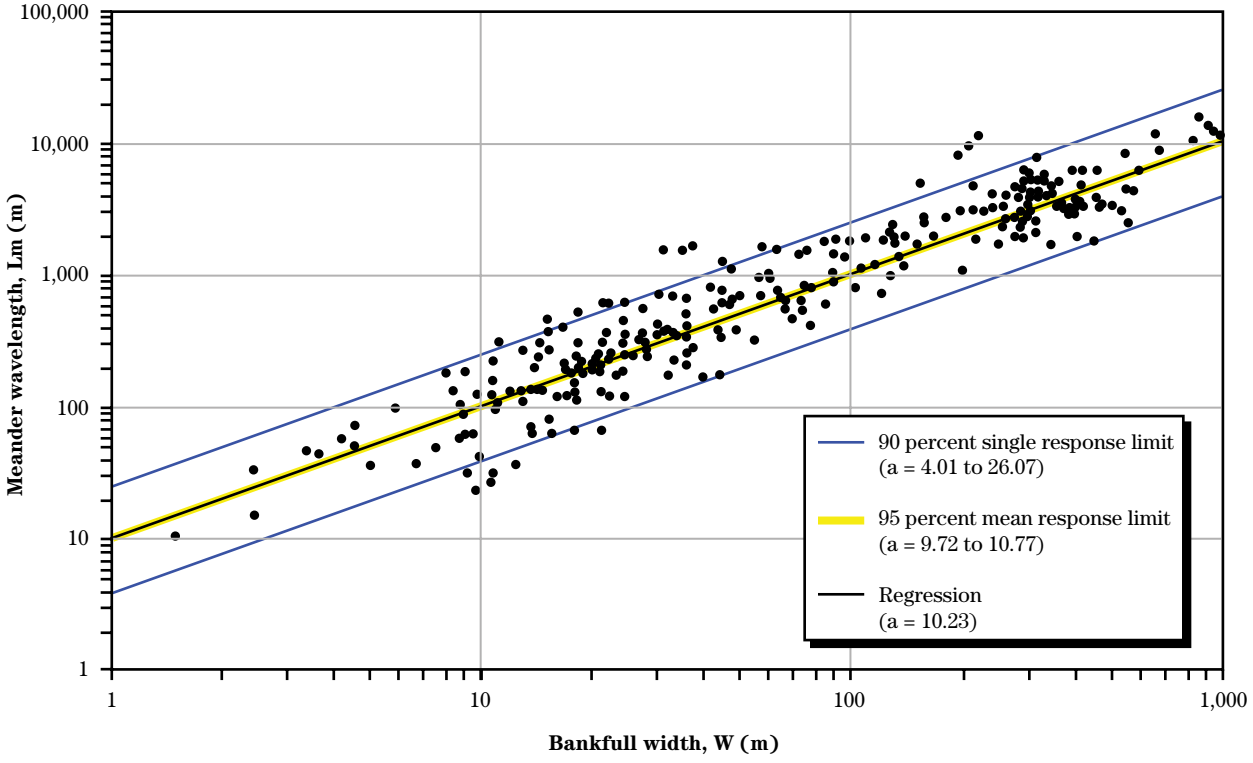

Table 12–1 Research and data sources for meander wavelengths

Researchers	Locations		No. of sites
Leopold and Wolman (1957)	United States rivers		21
Leopold and Wolman (1960)	Various sources	France	1
		United States	34
		Model river	1
		Total	36
Carlston (1965)	United States rivers		29
Schumm (1968)	Midwestern United States rivers		25
Chitale (1970)	Large alluvial rivers	Africa	1
		Canada	1
		India	16
		Pakistan	2
		United States	1
		Total	21
Williams (1986)	Various sources	Australia	2
		Canada	7
		Sweden	17
		Russia	1
		United States	16
		Model river	1
		Total	44
Thorne and Abt (1993)	Red River	1966	35
		1981	39
	Hydrographic surveys between Index, AR, and Shreveport, LA		1
		India	12
		Netherlands	1
		United Kingdom	48
		United States	18
		Total	154
Annable (1996)	Alberta, Canada		30
Cherry, Wilcock, and Wolman (1996)	United States rivers, predominantly sand bed		79

Leopold (1994) provided a hydraulic geometry relationship for meander wavelength as a function of both channel width and mean radius of curvature (fig 12–4 (FISRWG 1998)). His data include measurements from rivers, flumes, the Gulf Stream, and glaciers. He suggested that the relationships could be used to indicate stream instability if meander wavelength for a given stream did not plot closely to the predicted relationship.

Other hydraulic geometry relationships for meander wavelength from the literature are given in table 12–2.

Additional guidance for determining meander geometry, including wavelength, along channel bend length, meander belt width, radius of curvature, and sinuosity are provided in Leopold (1994).

The channel meander length is simply the meander wavelength times the valley slope divided by the channel slope.

$$\text{channel meander length} = \frac{\text{wavelength} \times \text{valley slope}}{\text{channel slope}} \quad \text{(eq. 12–4)}$$

Figure 12–4 Planform geometry relationships

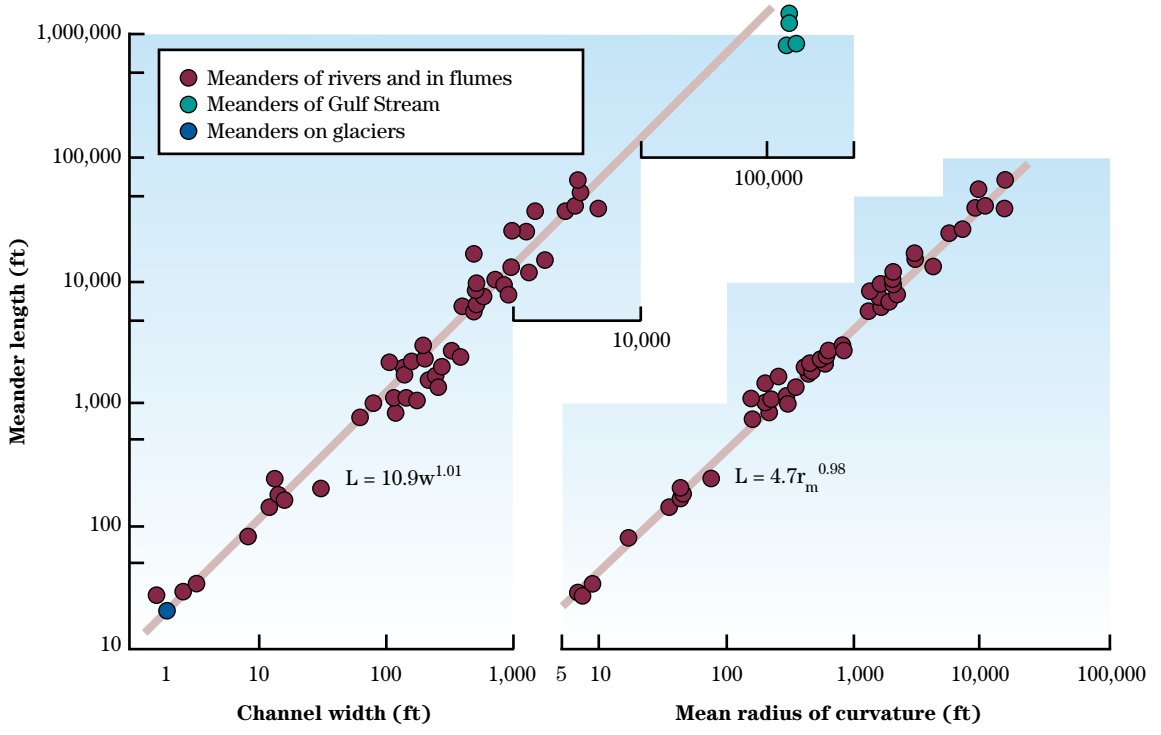

From Leopold (1994)

Table 12–2 Hydraulic geometry relationships for meander wavelength

Author	Equation	Units
Leopold and Wolman (1960)	$\lambda = 10.9\ W^{1.01}$	ft
Inglis (1941)	$\lambda = 6.06\ W^{0.99}$	ft
Yalin (1992)	$\lambda = 6\ W$	length
Dury (1965)	$\lambda = 30\ Q_{bf}^{0.5}$	ft, ft^3/s
Carlston (1965)	$\lambda = 8.2\ Q_{bf}^{0.62}$	ft, ft^3/s
Carlston (1965)	$\lambda = 106.1\ Q_{ma}^{0.46}$	ft^3/s
Schumm (1967)	$\lambda = 1890\ Q_{ma}^{0.34}\ M^{0.74}$	ft, ft^3/s

Notes: λ = meander wavelength
W = width
Q_{bf} = bankfull discharge
Q_{ma} = mean annual discharge
M = silt-clay factor

(b) Layout and sine-generated curve

Once meander wavelength is determined, planform can be determined using an analogy method or by using the sine-generated curve. Using a reference reach as a guide, planform can be laid on a map with a string cut to the appropriate channel length. Assuming that the planform can be approximated by the sine-generated curve is a more analytical approach and was suggested by Langbein and Leopold (1966). Their theory of minimum variance is based on the hypothesis that the river will seek the most probable path between two fixed points (the path that provides the minimum variance of bed shear stress and friction). The sine-generated curve is defined in figure 12–5 and by the following dimensionless equation:

$$\phi = \omega \cos \frac{2\pi s}{M} \qquad \text{(eq. 12–5)}$$

where:

ϕ = angle of meander path with the mean longitudinal axis (degrees or radians)
ω = maximum angle a path makes with the mean longitudinal axis (degrees or radians)
s = curvilinear coordinate along the meander path (ft or m)
M = meander arc length (ft or m)

The shape parameter, ω, is a function of the channel sinuosity, P, which can be solved by numerical integration, or may be approximated by the following equation (Langbein and Leopold 1966), in which ω is in radians:

$$\omega = 2.2\sqrt{\frac{P-1}{P}} \qquad \text{(eq. 12–6)}$$

The shape parameter of a sine-generated curve defines the shape of the stream as shown in figure 12–6 (Langbein and Leopold 1966).

Calculation of the points on a sine-generated curve is a rather tedious numeric integration for ϕ. However, the integration can be accomplished using a computer program such as the one in the U.S. Army Corps of Engineers (USACE) Hydraulic Design Package: SAM (Thomas, Copeland, and McComas 2003). The sine-generated curve produces a very uniform meander pattern. The alignments of natural channels are rarely perfect sinusoids. Channels that are constructed as such, therefore, appear strange. A combination of the string layout method and the analytical approach would produce a more natural looking planform.

Figure 12–5 Definition of sine-generated curve

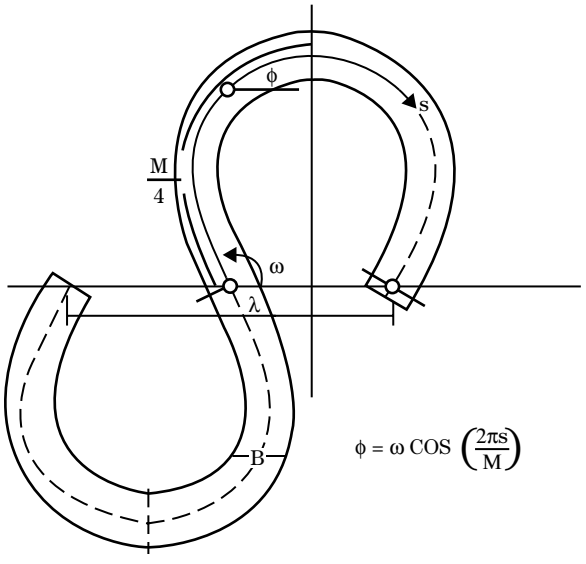

Figure 12–6 Effect of the shape factor on channel sinuosity with the sine-generated curve

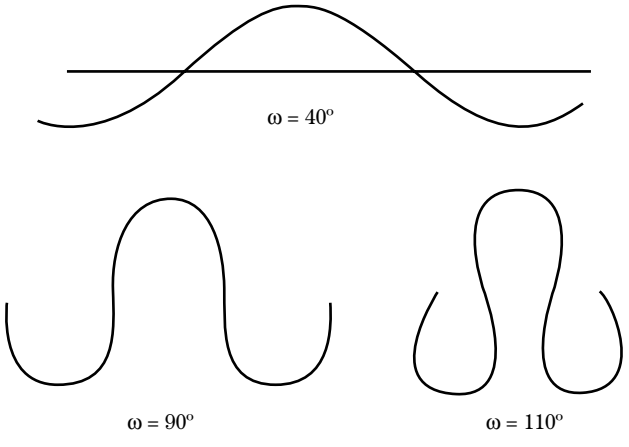

Example problem: Channel alignment

Objective: Determine the planform layout for the channel designed in the previous problem. Use the sine-generated curve.

Given:

Base width	=	80 ft
Depth	=	2.9 ft (at channel-forming discharge)
Side slopes	=	1V:2.5H
Channel slope	=	0.0050
Valley slope	=	0.0055

Solution:

Step 1 Calculate the top width of the channel for the channel-forming discharge.

$$TW = 2zy + BW$$

$$TW = (2)(2.5)(2.9) + 80 = 94.5 \text{ say } 95 \text{ ft}$$

Step 2 Determine the meander wavelength directly from figure 12–3 or from the mean regression equation for the meander wavelength (fig. 12–4). If figure 12–3 is used directly, the top width must be converted to meters (95 divided by 3.281 which equals 29 m). If the equations from figure 12–4 are used, the unit conversion is not needed because the regression equation is dimensionless.

$$\lambda = 10.23TW$$

$$\lambda = 10.23(95) = 972 \text{ ft}$$

Step 3 Determine the distance along the channel for one wavelength.

$$M = \frac{\lambda(\text{Valley slope})}{\text{Channel slope}}$$

$$M = \frac{972(0.0055)}{(0.0050)} = 1{,}069 \text{ ft}$$

Step 4 Calculate xy coordinates for the channel using a spreadsheet or the USACE Hydraulic Design Package, SAM (Thomas, Copeland, and McComas 2003). Input is wavelength, λ, and channel length, M. Output is shown in table 12–3. The calculated shape factor, ω, is 34.9 degrees. The calculated planform amplitude is 199 feet. A planform plot developed from the SAM output is shown in figure 12–7. Note that this planform is very regular and does not replicate natural meanders. The designer should use the sine-generated curve layout as a guide and manipulate the actual centerline layout based on site constraints.

Table 12–3 Output for hydraulic computations using the SAM model

```
*****************************************************************
* SAMwin Software Registered to the US Army Corps of Engineers  *
*****************************************************************
*                              HYDRAULIC CALCULATIONS           *
*                                   Version 1.0
* A Product of the Flood Control Channels Research Program      *
* Coastal & Hydraulics Laboratory, USAE Engineer R & D Center   *
*                                in cooperation with
*            Owen Ayres & Associates, Inc., Ft. Collins, CO     *
*****************************************************************
TABLE 1. LIST INPUT DATA.

T1 Gravel bed River Example
T1 Base width 80 ft
T1 Depth 2.9 ft
T1 Side Slopes 1V : 2.5H
T1 Top Width 95 ft
MG  972  1069
$$END

INPUT IS COMPLETE.
   ***********************************************************
   *
   *  PLANFORM GEOMETRY FOR A MEANDERING Sand bed STREAM
   *
   ***********************************************************

                                        MAXIMUM
   WAVE      MEANDER                   DEFLECTION
  LENGTH     LENGTH      SINUOSITY     ANGLE-DEG       AMPLITUDE
  972.00    1069.00        1.10         34.933          198.97

 COORDINATES ALONG ONE MEANDER WAVELENGTH

 ALONG THE       DEFLECTION       PERPENDICULAR TO      ALONG THE
  CHANNEL          ANGLE           VALLEY SLOPE       VALLEY SLOPE
                  DEGREES

     S              THETA              Y                  X

     0.00           34.93              0.00               0.00
    10.69           34.86              6.12               8.77
    21.38           34.66             12.21              17.55
    32.07           34.31             18.26              26.36
    42.76           33.84             24.25              35.22
    53.45           33.22             30.16              44.13
    64.14           32.48             35.96              53.11
```

Table 12–3 Output for hydraulic computations using the SAM model—Continued

S	THETA	Y	X
74.83	31.61	41.63	62.17
85.52	30.61	47.15	71.32
96.21	29.49	52.51	80.58
106.90	28.26	57.67	89.94
117.59	26.92	62.62	99.41
128.28	25.47	67.34	109.00
138.97	23.91	71.80	118.72
149.66	22.27	76.00	128.55
160.35	20.53	79.90	138.50
171.04	18.72	83.49	148.57
181.73	16.83	86.75	158.75
192.42	14.87	89.67	169.03
203.11	12.86	92.23	179.41
213.80	10.79	94.42	189.87
224.49	8.69	96.23	200.41
235.18	6.55	97.65	211.00
245.87	4.38	98.67	221.64
256.56	2.19	99.28	232.31
267.25	0.00	99.48	243.00
277.94	-2.19	99.28	253.69
288.63	-4.38	98.67	264.36
299.32	-6.55	97.65	275.00
310.01	-8.69	96.23	285.59
320.70	-10.79	94.42	296.13
331.39	-12.86	92.23	306.59
342.08	-14.87	89.67	316.97
352.77	-16.83	86.75	327.25
363.46	-18.72	83.49	337.43
374.15	-20.53	79.90	347.50
384.84	-22.27	76.00	357.45
395.53	-23.91	71.80	367.28
406.22	-25.47	67.34	377.00
416.91	-26.92	62.62	386.59
427.60	-28.26	57.67	396.06
438.29	-29.49	52.51	405.42
448.98	-30.61	47.15	414.68
459.67	-31.61	41.63	423.83
470.36	-32.48	35.96	432.89
481.05	-33.22	30.16	441.87
491.74	-33.84	24.25	450.78
502.43	-34.31	18.26	459.64
513.12	-34.66	12.21	468.45
523.81	-34.86	6.12	477.23

Table 12–3 Output for hydraulic computations using the SAM model—Continued

S	THETA	Y	X
534.50	-34.93	0.00	486.00
545.19	-34.86	-6.12	494.77
555.88	-34.66	-12.21	503.55
566.57	-34.31	-18.26	512.36
577.26	-33.84	-24.25	521.22
587.95	-33.22	-30.16	530.13
598.64	-32.48	-35.96	539.11
609.33	-31.61	-41.63	548.17
620.02	-30.61	-47.15	557.32
630.71	-29.49	-52.51	566.58
641.40	-28.26	-57.67	575.94
652.09	-26.92	-62.62	585.41
662.78	-25.47	-67.34	595.00
673.47	-23.91	-71.80	604.72
684.16	-22.27	-76.00	614.55
694.85	-20.53	-79.90	624.50
705.54	-18.72	-83.49	634.57
716.23	-16.83	-86.75	644.75
726.92	-14.87	-89.67	655.03
737.61	-12.86	-92.23	665.41
748.30	-10.79	-94.42	675.87
758.99	-8.69	-96.23	686.41
769.68	-6.55	-97.65	697.00
780.37	-4.38	-98.67	707.64
791.06	-2.19	-99.28	718.31
801.75	0.00	-99.48	729.00
812.44	2.19	-99.28	739.69
823.13	4.38	-98.67	750.36
833.82	6.55	-97.65	761.00
844.51	8.69	-96.23	771.59
855.20	10.79	-94.42	782.13
865.89	12.86	-92.23	792.59
876.58	14.87	-89.67	802.97
887.27	16.83	-86.75	813.25
897.96	18.72	-83.49	823.43
908.65	20.53	-79.90	833.50
919.34	22.27	-76.00	843.45
930.03	23.91	-71.80	853.28
940.72	25.47	-67.34	863.00
951.41	26.92	-62.62	872.59
962.10	28.26	-57.67	882.06
972.79	29.49	-52.51	891.42
983.48	30.61	-47.15	900.68

Table 12–3 Output for hydraulic computations using the SAM model—Continued

S	THETA	Y	X
994.17	31.61	-41.63	909.83
1004.86	32.48	-35.96	918.89
1015.55	33.22	-30.16	927.87
1026.24	33.84	-24.25	936.78
1036.93	34.31	-18.27	945.64
1047.62	34.66	-12.21	954.45
1058.31	34.86	-6.12	963.23
1069.00	34.93	0.00	972.00

Figure 12–7 Planform layout for one meander wavelength from sine-generated curve for example problem: wavelength = 972 ft; amplitude = 199 ft; sinuosity = 1.1

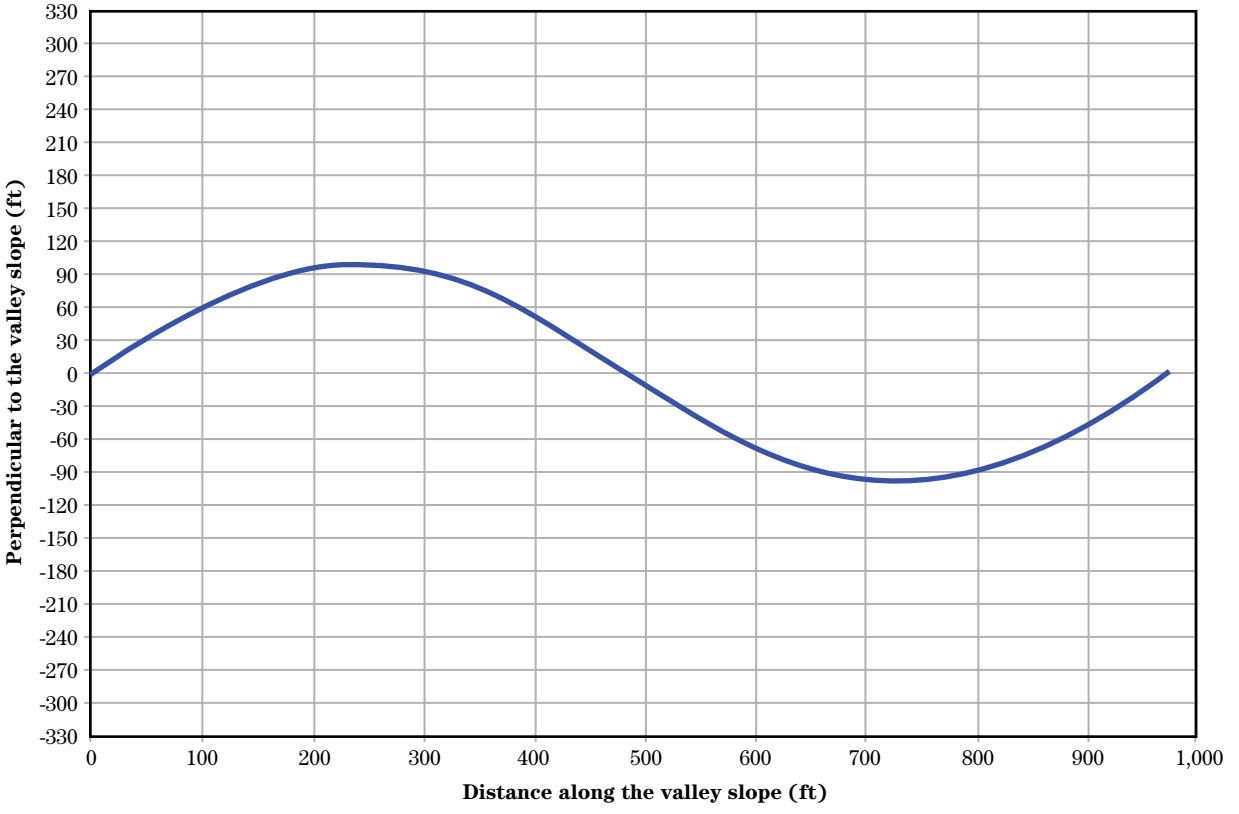

(c) Radius of curvature

The radius of planform curvature is not constant in the sine-generated curve, but ranges from a maximum value at the inflection point to a minimum curvature around the bend apex. The average radius of curvature is centered at the bend apex for a distance of approximately a sixth of the channel meander length.

Most reaches of stable meandering rivers have radius of curvature-to-width ratios between 1.5 and 4.5. Of the 438 sites used to derive the wavelength-width relationship in figure 12–3, radius of curvature is recorded for 263 of the sites. This subset was used to develop a cumulative distribution curve of radius of curvature-to width ratios (fig. 12–8). This figure shows that 33.5 percent, 52.9 percent, and 71.2 percent of the sites have radius of curvature-to-width ratios between 2 and 3, 2 and 4, and 1.5 and 4.5, respectively. The final planform layout should have ratios within the normal range.

If the calculated meander length is too large or if the required meander belt width is unavailable, grade control structures may be required to reduce the channel slope and stabilize the bed elevations.

Figure 12–8 Cumulative distribution of radius of curvature-to-width ratio derived from a composite data set of 263 sites

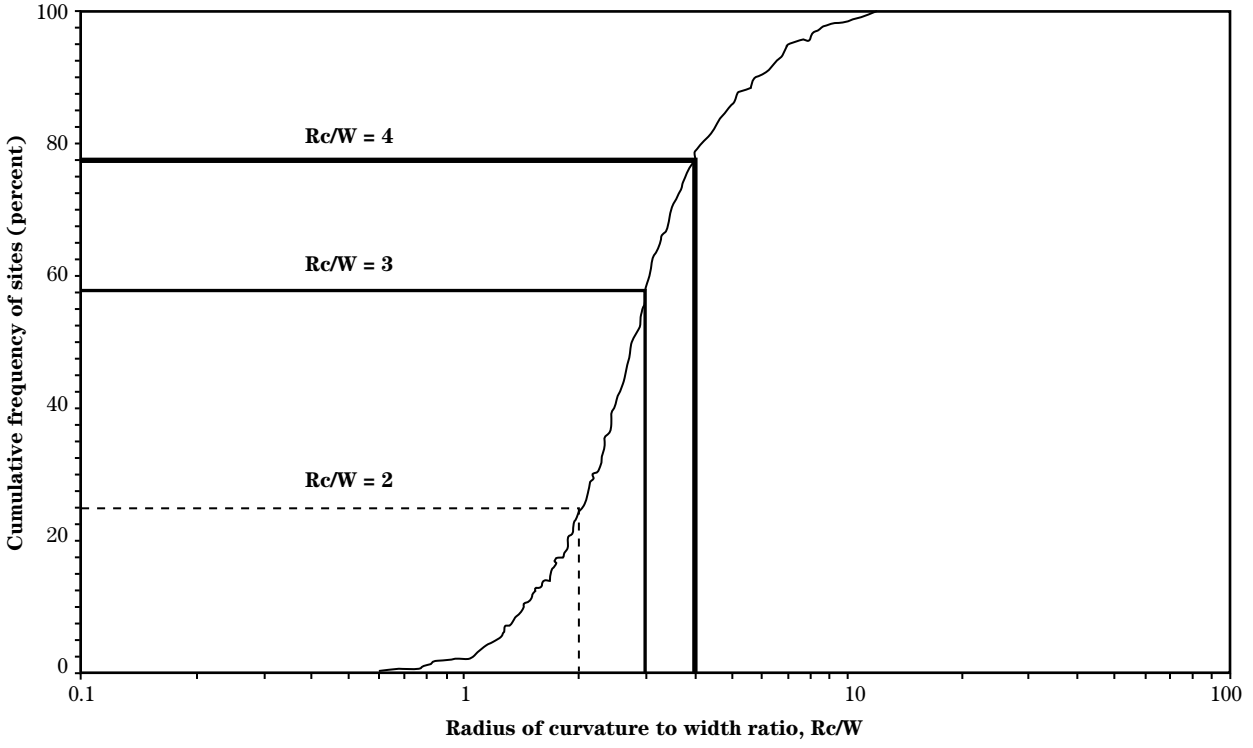

654.1203 Natural variability

Natural streams and rivers are rarely of uniform depth and width. Variability in channel width and depth can either be allowed to develop naturally or can be part of the project design. Sand-bed streams have the ability to create natural variability in channel form rather quickly because they are characterized by significant bed-material sediment transport. Gravel-bed streams typically adjust much more slowly. Streams with very little bed-material movement may not adjust at all. If variability is to be included in the project design, dimensions for cross sections in riffles and pools can be obtained from stable reaches of the existing stream or from reference reaches.

(a) Natural variability in width for gravel-bed rivers

Gravel-bed rivers are typically characterized by riffles and pools which correspond to bends and crossings in sand-bed rivers. In stable gravel-bed rivers, riffles are wider and shallower than the average channel width, and the pools tend to be deeper and somewhat narrower. In meandering gravel-bed rivers, the pools tend to be in the bends and the riffles at the inflection points. In the design of gravel-bed channels, the natural variability in cross-sectional width can be estimated using hydraulic geometry relationships or reference reaches. As with all hydraulic geometry and analogy methods, the design tools should be developed from physiographically similar watersheds.

Hey and Thorne (1986) developed hydraulic geometry relationships for meandering gravel-bed rivers in the United Kingdom. Their regression equations were based on surveys from 62 stable self-formed channels in erodible material with well-defined flood plains. At most sites, the banks were either cohesive or composite. Composite banks are defined as noncohesive sand and gravel layers overlain by a cohesive layer. These sites include the range of data used in developing the regression equations that are described in more detail in NEH654.09. A typical example of one of the Hey and Thorne rivers is shown in figure 12–9.

Riffle spacing and riffle width are determined from regression equations as a function of the mean channel width. The mean channel width is determined from one of three hydraulic geometry relationships described in NEH654.09. The Hey and Thorne hydraulic geometry relations for mean width consider the density of vegetation along the channel banks. The equations for riffle spacing are applicable for all bank conditions. The riffle spacing is given as a function of mean width:

$$Z = 6.31W \qquad \text{(eq. 12–7)}$$

where:
Z = the riffle spacing
W = the mean channel top width

Most of the data fell between the equations as shown in figure 12–10.

$$Z = 10W \qquad \text{(eq. 12–8)}$$

$$Z = 4W \qquad \text{(eq. 12–9)}$$

Riffle spacing tends to be nearer 4 channel widths on steeper gradients, increasing to 10 channel widths with more gradual slopes.

The riffle mean width, RW, was given as:

$$RW = 1.034W \qquad \text{(eq. 12–10)}$$

Hey and Thorne's riffle widths varied between 1.5W and 0.75 W.

Figure 12–9 Typical British gravel-bed river used in Hey and Thorne (1986) study

Figure 12–10 Relation between riffle spacing, Z, and bankfull channel width, W

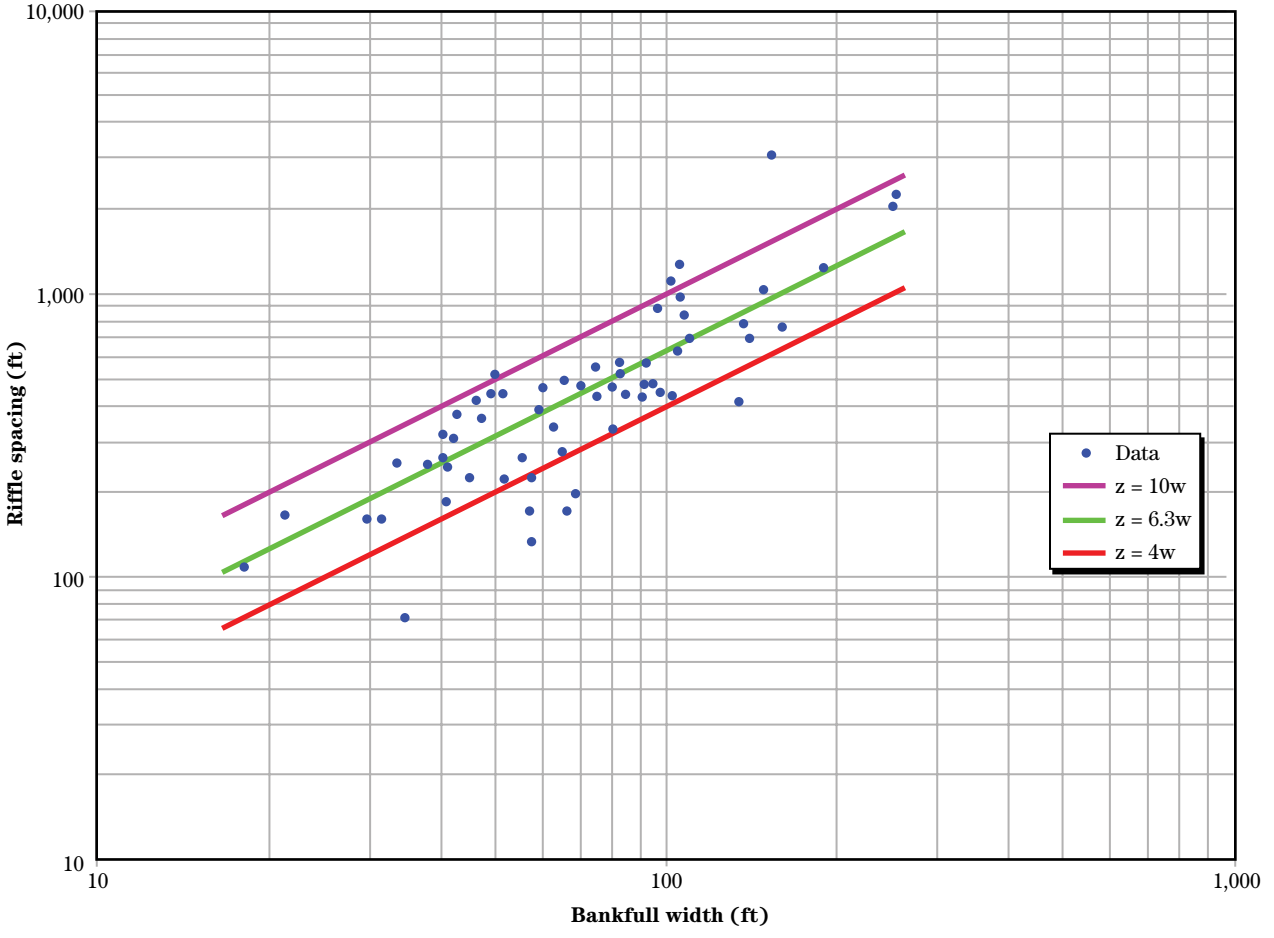

(b) Riffle and pool spacing in nearly straight rivers

In rivers that are nearly straight (sinuosity less than 1.2), riffle and pool spacing may be set as a function of channel width. The empirical guide of 5 to 7 channel widths applies here (Knighton 1984). Two times this riffle spacing gives the total channel length through one meander pattern.

(c) Natural variability around meander bendways

Thorne (1988) and Thorne and Soar (2001) compiled empirical data sets of cross-sectional and planform dimensions from meander bends in the Red River between Index, Arkansas, and Shreveport, Louisiana. The Red River in this reach is typical of relatively large meandering rivers, with a wide variety of both bend geometries and bank materials. These studies provided a useful baseline database for examining the variability of width around meander bends, location of pools, and maximum pool depths. Equations were developed to define natural variability around the meander bends. Of course, if applied elsewhere, these equations should be used with caution.

The bends in the Red River data set were classified as one of three types based on the Brice (1975) classification system: equiwidth meanders, denoted as Type e (T_e) meanders (fig. 12–11); meanders with point bars, denoted as Type b (T_b) meanders (fig. 12–12); and meanders with point bars and chute channels, denoted as Type c (T_c) meanders (fig. 12–13). The Red River meander bend geometry data set is shown in table 12–4.

- **Equiwidth meandering**—Equiwidth indicates that there is only minor variability in channel width around meander bends. These channels are generally characterized by low width-to-depth ratios, erosion resistant banks, fine-grain bed material (sand or silt), low bed-material load, low velocities, and low stream power. Channel migration rates are relatively low because the banks are naturally stable.
- **Meandering with point bars**—Meandering with point bars refers to channels that are significantly wider at bendways than crossings, with well-developed point bars, but few chute channels. These channels are generally

Figure 12–11 Equiwidth meandering river, Type e (T_e)

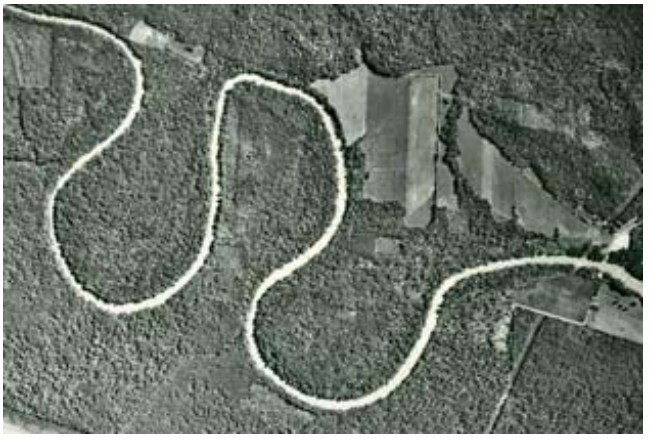

Figure 12–12 Meandering with point bars, Type b (T_b)

Figure 12–13 Meandering with point bars and chute channels, Type c (T_c)

characterized by intermediate width-to-depth ratios, moderately erosion-resistant banks, medium-grained bed material (sand or gravel), medium bed-material load, medium velocities, and medium stream power. Channel migration rates are likely to be moderate unless banks are stabilized.

- **Meandering with point bars and chute channels**—Meandering with point bars and chute channels refers to channels that are much wider at bendways than crossings, with well-developed point bars and frequent chute channels. These channels are generally characterized by moderate to high width-to-depth ratios, highly erodible banks, medium to coarse-grained bed material (sand, gravel and/or cobbles), heavy bed-material load, moderate to high velocities, and moderate to high stream power. Channel migration rates are likely to be moderate to high unless banks are stabilized.

Ranges of physical characteristics pertaining to each of the meander bend types are addressed in more detail in NEH654.09. Figure 12–14 provides a definition sketch for channel cross-sectional geometries and dimensions through a meander.

Table 12–4 Ranges of physical characteristics found in different meander bend types identified from the 1981 Red River hydrographic survey between Index, AR, and Shreveport, LA

	n	S (10^6)	P	W_i / d_m	d_{max} / d_i	Rc / W_i
Type e	20 (8)	65 to 268 (133 to 268)	1.0 to 2.1 (1.2 to 2.1)	34.2 to 74.1 (38.3 to 74.1)	1.6 to 2.4 (1.7 to 2.4)	0.9 to 9.3 (0.9 to 5.2)
Type b	34 (19)	76 to 294 (105 to 294)	1.0 to 2.0 (1.1 to 2.0)	36.8 to 121.0 (36.8 to 102.4)	1.5 to 2.6 (1.7 to 2.6)	1.5 to 9.1 (1.5 to 6.1)
Type c	13 (10)	91 to 201 (91 to 201)	1.1 to 2.3 (1.2 to 2.3)	33.5 to 88.2 (33.5 to 88.2)	1.6 to 2.4 (1.6 to 2.4)	2.2 to 6.8 (2.2 to 5.2)

Note:
n = number of meander bends studied
S = water surface slope
P = sinuosity
W_i / d_m = inflection point width-to-mean depth ratio
d_{max} / d_i = maximum scour depth in pool-to-mean depth at inflection point
Rc / W_i = radius of curvature-to-inflection point width ratio
Values in parentheses refer to meander bends with sinuosity 1.2 or greater.

Figure 12–14 Meander cross-sectional dimensions for variability design

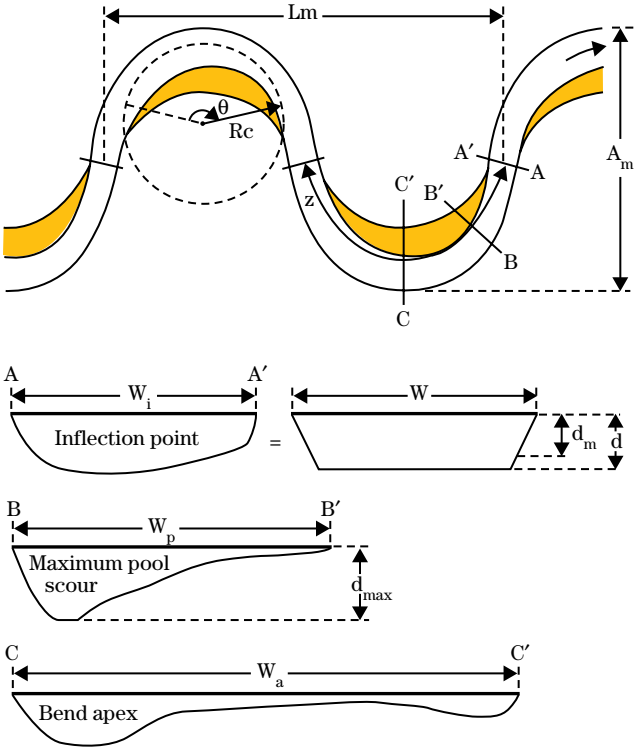

Note: Point bars defined by shaded regions

Lm	=	meander wavelength	Z	=	meander arc length (riffle spacing)
A_m	=	meander belt width	Rc	=	radius of curvature
θ	=	meander arc angle	W	=	reach average bankfull width
d	=	depth of trapezoidal cross section	d_m	=	mean depth (cross-sectional area / W)
d_{max}	=	maximum scour depth in bendway pool	W_i	=	width at meander inflection point
W_p	=	width at maximum scour location	W_a	=	width at meander bend apex

(d) Width variability around meander bends

Two dimensionless parameters can be used to describe the width variability around meander bends, based on the enhanced Red River data set. These are the ratio of bend apex width to inflection point width, W_a/W_i, and the ratio of width at the location of maximum bend pool scour to inflection point width, W_p/W_i. Theoretically, these parameters adjust according to the degree of curvature and the type of meander bend. To derive new morphological relationships, sinuosity, P, was preferred as the independent variable, rather than the radius of curvature-to-width ratio. The latter would have resulted in width appearing on both sides of the regression equations.

Morphologic relationships for the width ratios as a function of meander type were developed for channels with sinuosities greater than 1.2. This is a commonly accepted threshold between nearly straight channels with only slight sinuosity and meandering channels with moderate to high sinuosity. The bed apex width to the inflection point width ratio, W_a/W_i, was found to be independent of sinuosity. Data are plotted with confidence limits in figure 12–15. Values for the ratios for each type of meander bend can be determined from table 12–5 and the following equation, where p denotes the level of significance and corresponds to the 100(1–p) percent confidence level.

Morphologic relationships for the width ratios as a function of meander type were developed for the ratio of pool width at the location of maximum scour to inflection point width (W_p/W_i) for channels with sinuosities greater than 1.2. This ratio was also found to be independent of sinuosity. Data and confidence limits are plotted in figure 12–16 (source data: 1981 Red River hydrographic survey). Values for the ratios for each type of meandering river can be determined from the following equation and table 12–6.

$$\left(\frac{W_a}{W_i}\right)_p = a + u_p \qquad \text{(eq. 12–11)}$$

Figure 12–15 Ratio of bend apex width to inflection point width, W_a/W_i as a function of meander bend type only, for sinuosities of at least 1.2. Confidence limits of a mean response are shown at the 95 percent level. (Source data: 1981 Red River hydrographic survey)

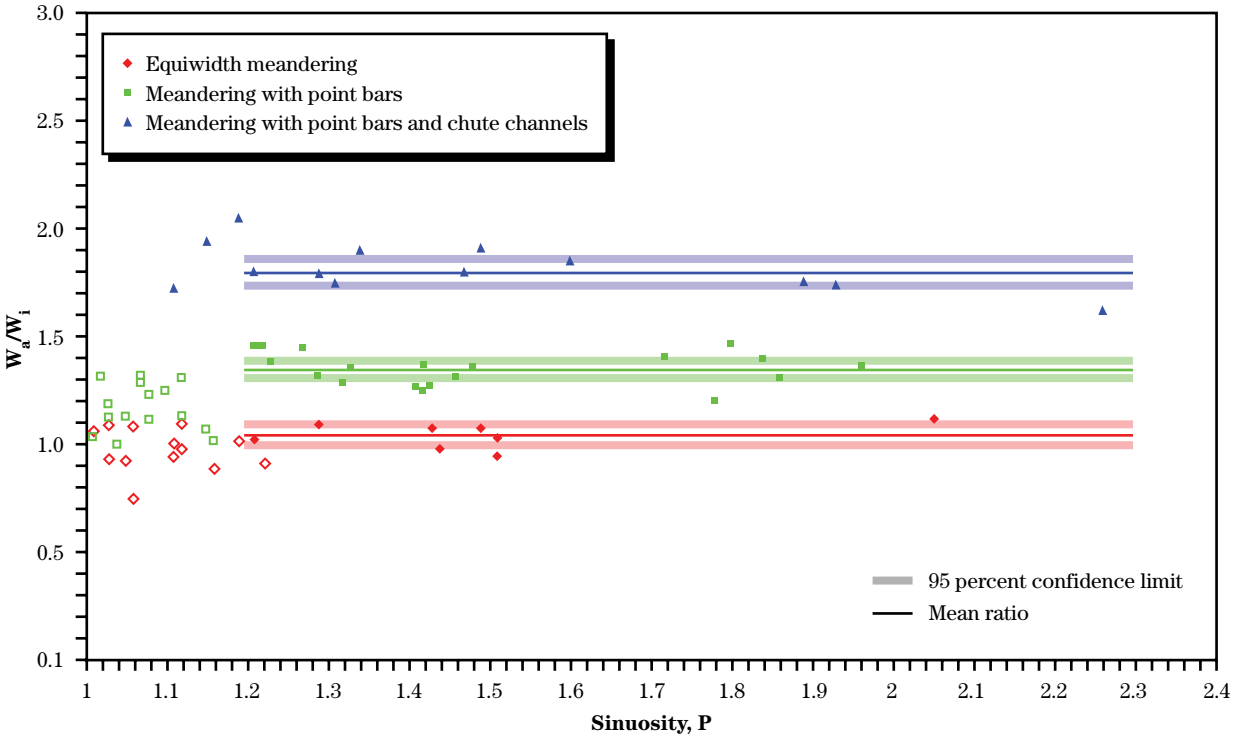

Note: Filled symbols = sinuosity of at least 1.2; empty symbols = sinuosity less than 1.2

Table 12–5 Constant values used to estimate the mean ratio of bend apex width to inflection point width, W_a/W_i, within confidence bands for different types of meander bends and for sites with sinuosity of at least 1.2. Coefficients pertaining to the 99, 95, and 90 percent confidence limits are given.

	a	$u_{0.01}$	$u_{0.05}$	$u_{0.1}$
Type e	1.05	0.08	0.05	0.04
		(0.29)	(0.20)	(0.16)
Type b	1.35	0.05	0.04	0.03
		(0.27)	(0.20)	(0.16)
Type c	1.79	0.09	0.06	0.05
		(0.36)	(0.25)	(0.20)

Note: Values given refer to mean response confidence limits. Values in parentheses are used to calculate single response confidence limits.

Figure 12–16 Ratio of pool width (at maximum scour location) to inflection point width, W_p/W_i as a function of meander bend type only, for sinuosities of at least 1.2. Confidence limits of a mean response are shown at the 95 percent level.

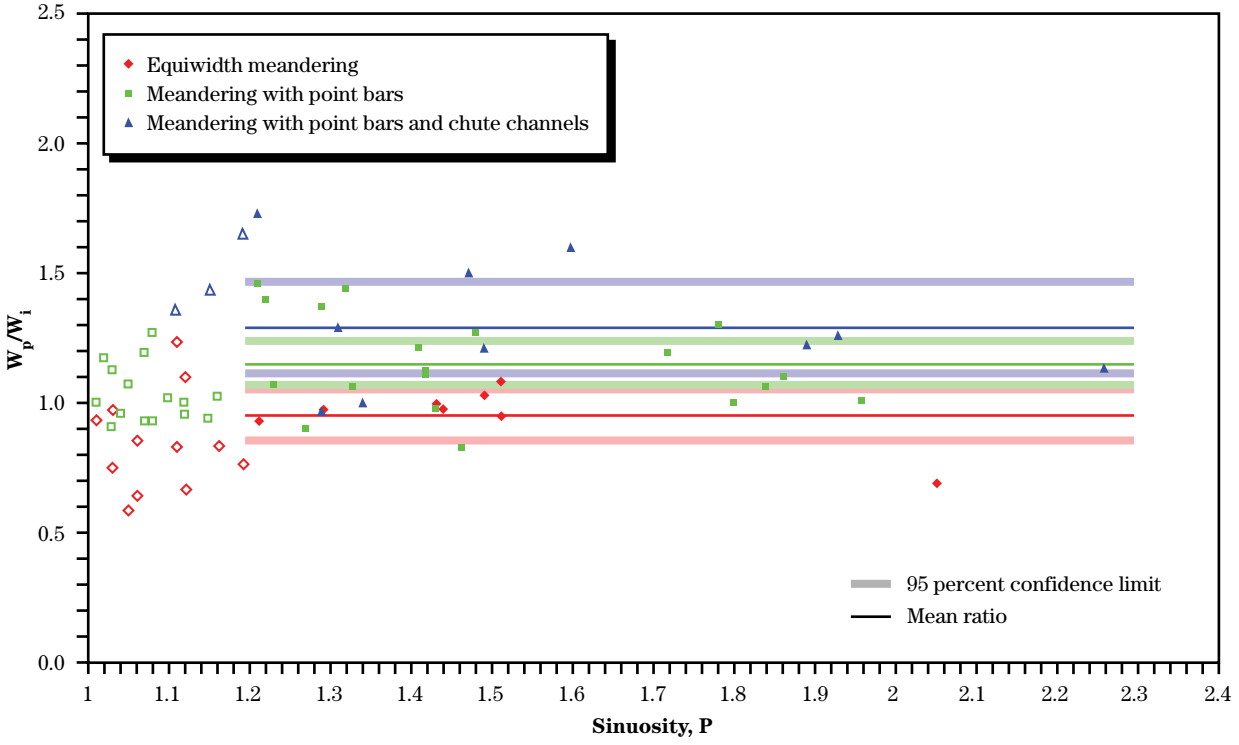

Note: Filled symbols = sinuosity of at least 1.2 empty symbols = sinuosity less than 1.2

Table 12–6 Constant values used to estimate the mean ratio of pool width (at maximum scour location) to inflection point width, W_p/W_i, within confidence bands for different types of meander bends and for sites with sinuosity of at least 1.2. Coefficients pertaining to the 99, 95, and 90 percent confidence limits are given.

	a	$u_{0.01}$	$u_{0.05}$	$u_{0.1}$
Type e	0.95	0.15	0.10	0.08
		(0.56)	(0.38)	(0.30)
Type b	1.15	0.12	0.09	0.07
		(0.64)	(0.47)	(0.39)
Type c	1.29	0.26	0.18	0.14
		(1.07)	(0.74)	(0.60)

Note: Values given refer to mean response confidence limits. Values in parentheses is used to calculate single response confidence limits.

(e) Location of the pool in a meander bend

While the location of meander inflection points and bend apexes are geometrically defined, the location of pools, defined by the position of maximum bend scour, is variable. Pool location is controlled by the meander configuration, complex velocity distribution, and large-scale coherent flow structures which pulse sediment along the channel to form alternate zones of scour and fill. In natural meanders, the deepest pool is usually located downstream from the bend apex. The pool location in a meander bend can be represented empirically by a pool-offset ratio, defined as the ratio of the channel distance between bend apex and maximum scour location to the channel distance between bend apex and downstream inflection point, Z_{a-p} / Z_{a-i}. The pool–offset ratio was found to be independent of sinuosity. Neither was a distinct relationship found for the different meander types. The range and cumulative distribution function for the pool-offset ratio is shown in figure 12–17 (source data: 1981 Red River hydrographic survey). The mean value for the ratio was 0.36 and the range was –0.4 to 1.08.

(f) Maximum scour in bendways

Maximum scour depth is calculated to incorporate deep pools in constructed channels and to estimate required toe depths for bank protection. Data from a wide range of rivers (Thorne and Abt 1993; Maynord 1996) were used to develop morphological equations for the maximum scour depth in pools. These maximum scour depths are based on the surveyed maximum local depth at the bend. The data were divided into two subsets using a width-to-depth threshold value of 60, which is an approximate modal value.

Figure 12–17 Cumulative distribution of the pool-offset ratio, Z_{a-p}/Z_{a-i}, for all types of meander bends studied. Confidence limits on the mean response are shown.

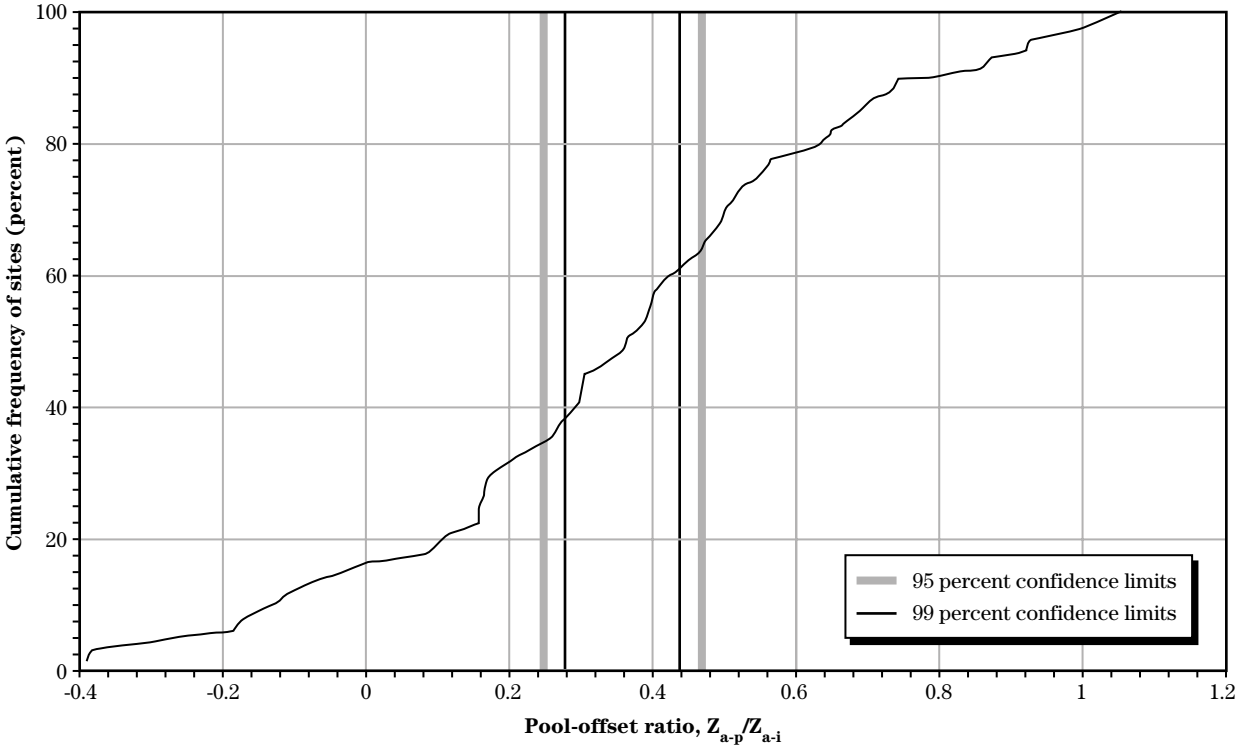

The best-fit morphological relationships are given by Thorne and Soar (2001) as:

$$\frac{W_i}{d_m} < 60 \qquad \text{(eq. 12–12)}$$

$$\frac{d_{max}}{d_m} = 2.14 - 0.19 \ln\left(\frac{Rc}{W_i}\right) \qquad \text{(eq. 12–13)}$$

$$\frac{W_i}{d_m} \geq 60 \qquad \text{(eq. 12–14)}$$

$$\frac{Rc}{W_i} < 10 \qquad \text{(eq. 12–15)}$$

$$\frac{d_{max}}{d_m} = 2.98 - 0.54 \ln\left(\frac{Rc}{W_i}\right) \qquad \text{(eq. 12–16)}$$

A practical, safe design curve may then be defined by considering both equations as:

$$\frac{d_{max}}{d_m} = 1.5 + 4.5\left(\frac{Rc}{W_i}\right)^{-1} \qquad \text{(eq. 12–17)}$$

This equation is an asymptotic relationship with a theoretical minimum d_{max}/d_m of 1.5, representing pool scour depths expected in a straight channel with a pool-riffle bed topography. From this upper-bound relationship, d_{max}/d_m ranges from 4 to 3 for Rc/W_i between 1.8 and 3. For channels with an Rc/W_i less than 1.8, pool depth is independent of bend curvature. The recommended dimensionless scour depth should be 4. All three relationships are portrayed in figure 12–18 (Thorne and Abt 1993; Maynord 1996), which show that this equation is a safe curve for both classes of W_i/d_m. More information on scour and how it relates to specific project features is provided in NEH654.14.

Figure 12–18 Dimensionless maximum scour depth in meander pools as a function of radius of curvature-to-width ratio

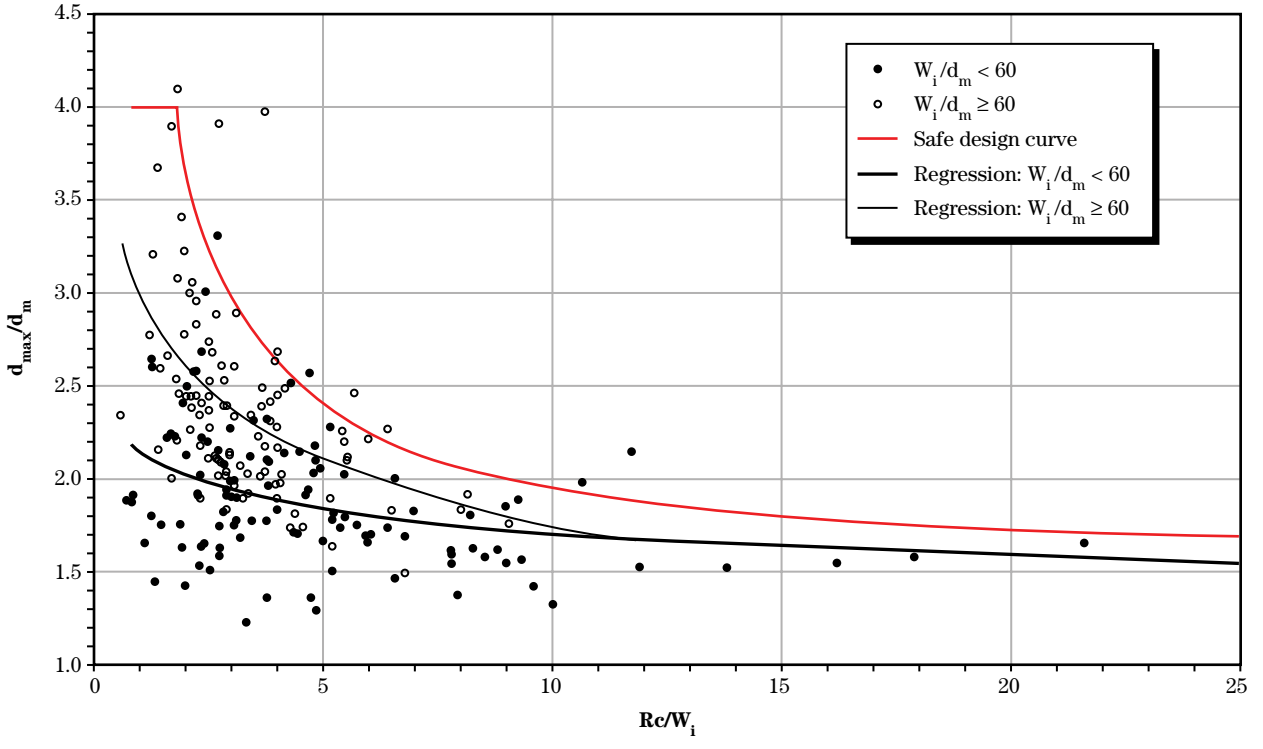

654.1204 Practical channel design equations for meander bend geometry

It is possible to derive a mean band of uncertainty, u, suitable for all three types of meander bends and to provide a set of practical design equations. The cumulative effects of Type e, Type b, and Type c bends are represented by the binary parameters, T_e, T_b and T_c, respectively. The value of T_e has a value of 1 for all three types of bend and represents the smallest planform width ratio. If point bars are present, but chute channels are rare, T_b is assigned a value of 1, and T_c is assigned a value of 0. If point bars are present and chute channels are common, both T_b and T_c are assigned values of 1. Obviously T_c can only be given a value of 1 when T_b has a value of 1.

Bend apex ($P \geq 1.2$)

$$\frac{W_a}{W_i} = 1.05T_e + 0.30T_b + 0.44T_c \pm u \qquad \text{(eq. 12–18)}$$

Pool width ($P \geq 1.2$)

$$\frac{W_p}{W_i} = 0.95T_e + 0.20T_b + 0.14T_c \pm u \qquad \text{(eq. 12–19)}$$

For all three bend types and sinuosities greater than 1, the pool offset ratio is given by:

Pool-offset ($P>1.0$)

$$\frac{Z_{a-p}}{Z_{a-i}} = 0.36 \pm u \qquad \text{(eq. 12–20)}$$

Values of u refer to confidence limits on the mean response as given in table 12–7.

A practical design equation for predicting or constructing maximum scour depths at bends is the upper-bound curve in figure 12–17, given by the following equation:

$$\frac{d_{max}}{d_m} = 1.5 + 4.5\left(\frac{R_c}{W_i}\right)^{-1} \qquad \text{(eq. 12–21)}$$

For sites where active meandering is not permitted, bank protection will be required along the outer bank to prevent erosion. In addition, this equation should be used together with bank stability charts to establish whether bank stabilization against mass failure is also necessary.

Table 12–7 Uncertainty, u, in estimates of width variability around meander bends and location of pools. Values refer to confidence limits on the mean response.

Confidence limits %	W_a / W_i	W_p / W_i	Z_{a-p} / Z_{a-i}
99	0.07	0.17	0.11
95	0.05	0.12	0.08
90	0.04	0.10	0.07

654.1205 Bankline migration

Bankline migration is a natural process associated with natural meandering channels. Meander loops tend to move downstream as river processes erode the outside of bends and deposit sediment on point bars. The ability to forecast adjustments in planform is important to the planning and design of any project where highways or structures could be damaged. The rate of bank migration at a given site is a function of erosional forces and resisting forces. The variables affecting erosional forces include discharge, cross-sectional geometry, sediment load, bed roughness, bedforms and bars, and the geometry of the bend itself. The variables affecting resistance forces include bank geometry, the composition of the bank, bank vegetation, pore water pressure, freezing and thawing, and wetting and drying. Due to the wide variability in significant variables, it is difficult to develop an algorithm that can reliably predict bankline migration rates.

Nanson and Hickin (1986) compiled data for 18 gravel-bed rivers in western Canada and reported maximum bankline migration rates at the bend apex (fig. 12–19). Cherry, Wilcock, and Wolman (1996) used 133 data sets from meandering sand-bed rivers collected by James Brice of the USGS to develop an empirical relationship to estimate bankline migration. They related mean annual flow and channel width to the mean erosion rate along the entire length of channel (fig. 12–20). They concluded that the simple correlation was inadequate. However, it does provide an order of magnitude estimate for the mean erosion rate and can be used to estimate a range of probable erosion rates.

Figure 12–19 Bankline migration rates in gravel-bed rivers

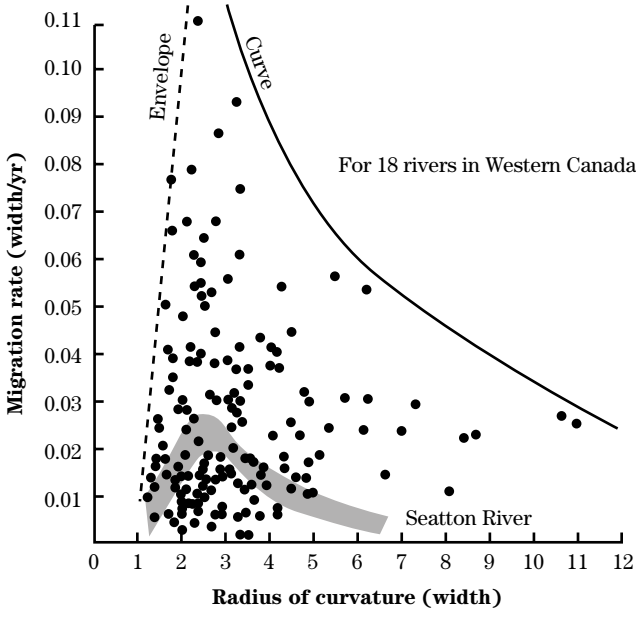

Figure 12–20 Average bank erosion rate

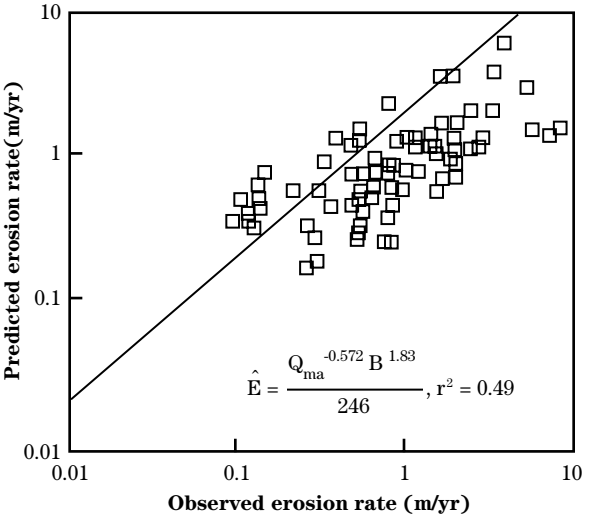

Figure 12–21 Modified Brice classification system for estimating bankline migration

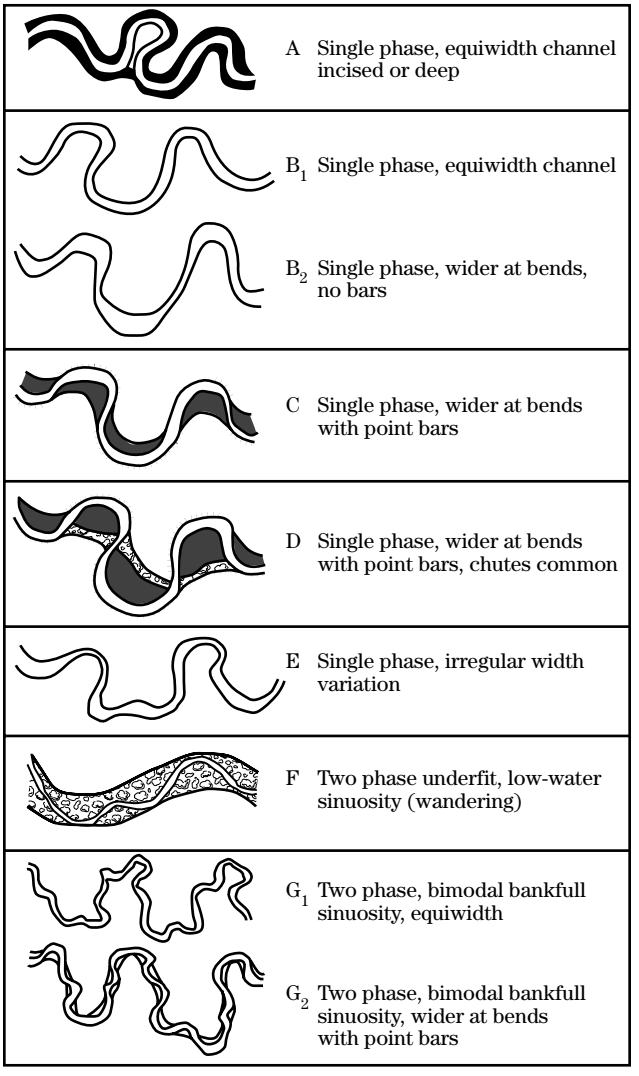

Ayres Associates (2004) used the same data set as Cherry, Wilcock, and Wolman (1996), relating the maximum rate of apex movement to the channel width at the apex. They segregated the data for four channel types: B1–single phase equiwidth, B2–single phase wider at bends, C–single phase with point bars, and A–single phase incised or deep. Their classification is a modification of the Brice (1975) classification system shown in figure 12–21 (Ayers Associates 2004). The scatter in the Ayres data (fig. 12–22 is about the same. Note that the Cherry, Wilcock, and Wolman (1996) data and bank migration rates can only be estimated in an approximate sense. Ayres Associates plotted a cumulative percentage of apex movement curve (fig. 12–23) which provides a useful tool for predicting bankline migration in terms of risk and uncertainty.

Several researchers have developed two-dimensional, depth-averaged numerical models to predict bankline migration. These models are data intensive and should be considered research tools. Garcia, Bittner, and Nino (1994) related the local erosion rate to the difference in the average velocity and the near-bank velocity. Odgaard (1986) related erosion to the difference in average depth and near-bank depth. The models produce relatively accurate velocity distributions in the meandering channel; however, bank resistance coefficients must be empirically determined or calibrated to existing conditions at specific sites. The high degree of variability in bank composition in meandering alluvial systems makes application of these models difficult.

The most reliable method for predicting bankline migration rate is to estimate historical rates from aerial photos of the project river. It must be recognized that rates at a specific site will change as the planform changes. In addition, erosion rates change with cyclic climate changes and changes in the watershed.

Figure 12–22 Bankline migration—apex movement versus channel width

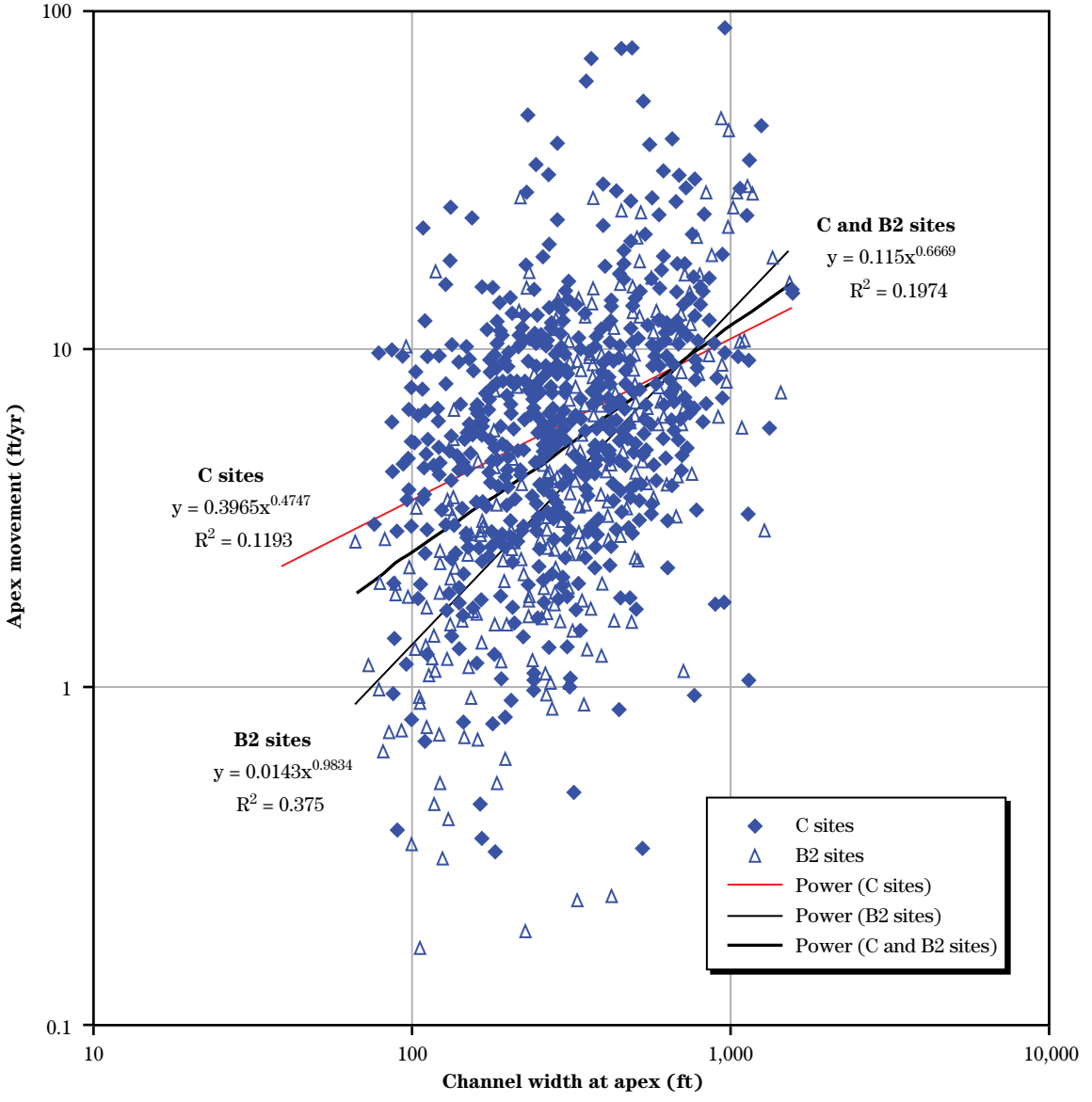

Figure 12–23 Cumulative percentage of apex bend movement

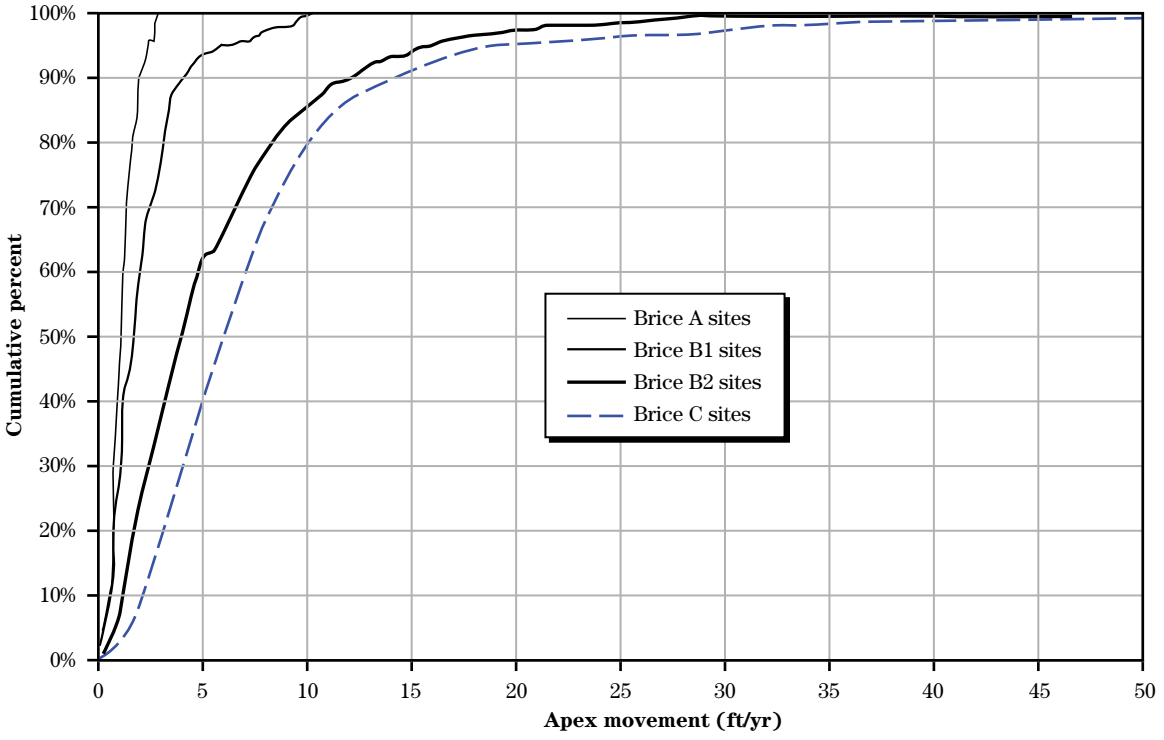

Example problem: Variability in channel planform geometry

Objective: Average channel dimensions for a new meandering sand-bed channel with point bars have been determined. Provide for channel geometry variability so that the new channel will not have excessive adjustments to make as it seeks its new equilibrium condition. Determine the channel width at the bend apex and at the location of the maximum scour. Also, estimate the most probable maximum scour depth and its most probable location. Determine the design depth of the bank protection if it is needed. Estimate the bankline migration rate that might occur if the bank is not protected.

Given: Average channel dimensions at the crossing and the general planform alignment are:

Width = 450 ft
Depth = 25 ft
Channel slope = 0.00030
Valley slope = 0.00049
Meander wavelength = 5,000 ft
Radius of curvature = 2,000 ft
Channel-forming discharge = 50,000 ft^3/s
Mean annual flow = 8,000 ft^3/s

Step 1 Calculate sinuosity

$$P = \frac{\text{Valley slope}}{\text{Channel slope}}$$

$$P = \frac{0.00049}{0.00030} = 1.63$$

Step 2 Calculate the channel distance through one meander wavelength

$$M = P \times \text{ meander wave length}$$

$$M = 1.63 \times 5,000 = 8,150 \text{ ft}$$

Step 3 Calculate the channel width at the bend apex and at the pool using tables 12–5 and 12–6.

This is a type b channel (meandering with point bars)

Width at apex = 1.35 × average channel width

Width at apex = 1.35 × 450 ft

Width at apex = 608 ft

With 90 percent confidence that the width should be between

$$\text{Width at apex} = (1.35 + 0.16)$$

$$\text{and } (1.35 - 0.16) \times 450 = 680 \text{ and } 536 \text{ ft}$$

Width at pool = 1.15 × average channel width

Width at pool = 1.15 × 450 ft

Width at pool = 518 ft

With 90 percent confidence that the width should be between

$$\text{Width at pool} = (1.15 + 0.39)$$

$$\text{and } (1.15 - 0.39) \times 450 = 693 \text{ and } 356 \text{ ft}$$

Step 4 Determine the most probable location of the pool in bend using figure 12–17.

At a cumulative frequency of 50 percent (most probable) the pool-offset ratio is 0.36

$$\frac{Z_{a-p}}{Z_{a-i}} = 0.36$$

The distance to the bend apex from the crossing (inflection point) is one half the channel distance through a meander wavelength.

$$Z_{a-i} = \frac{M}{2} = \frac{8,150}{2} = 4,075 \text{ ft}$$

$$Z_{a-p} = 0.36 \times 4,075 = 1,467 \text{ ft}$$

The location of the pool is then 5,542 feet downstream from the inflection point.

$$4,075 + 1,467 = 5,542 \text{ ft}$$

Step 5 Determine the most probable scour depth and the safe design depth for bank protection using figure 12–18.

$$\frac{\text{Radius of curvature}}{\text{Average width}} = \frac{2,000 \text{ ft}}{450 \text{ ft}} = 4.44$$

$$\frac{\text{Average width}}{\text{Mean depth}} = \frac{450 \text{ ft}}{25 \text{ ft}} = 18$$

Calculate the average depth of scour at the pool.

$$\frac{d_{max}}{d_m} = 2.14 - 0.19 \ln\left(\frac{Rc}{W_i}\right)$$

$$d_{max} = 25\left[2.14 - 0.19 \ln\left(\frac{2{,}000 \text{ ft}}{460 \text{ ft}}\right)\right]$$

$$d_{max} = 46 \text{ ft}$$

Calculate the safe design depth for bank protection.

The mean depth should represent the depth at channel-forming discharge to set an average pool depth for the initial channel geometry, but should represent depth at a design frequency flood peak to set a design depth for bank protection. In this example, a wide flood plain is assumed so that channel-forming and flood depths are similar.

$$\frac{d_{max}}{d_m} = 1.5 + 4.5\left(\frac{Rc}{W_i}\right)^{-1}$$

$$d_{max} = 25 \text{ ft}\left[.5 + 4.5\left(\frac{450 \text{ ft}}{2{,}000 \text{ ft}}\right)\right]$$

$$d_{max} = 63 \text{ ft}$$

Step 6 Estimate bankline migration rate using the Cherry, Wilcock, and Wolman equation (fig. 12–20) and the Ayres Associates graph for a type C channel (fig. 12–21).

$$E = \frac{Q_{ma}^{-0.572} B^{1.83}}{246}, \; r^2 = 0.49$$

$$Q_{ma} = \frac{8{,}000}{35.3} = 227 \text{ m}^3/\text{s}$$

$$B = \frac{450 \text{ ft}}{3.28 \text{ ft/m}} = 137 \text{ m}$$

$$E \text{ m/yr} = \frac{\left(227^{-0.572} \times 137^{1.83}\right)}{246} = 1.5 \text{ m/yr} = 4.9 \text{ ft/yr}$$

Apex movement (ft/yr)= $0.3965W^{0.4747}$ ft

$$\text{Apex movement} = 0.3965(450)^{0.4747}$$

Apex movement = 7.2 ft/yr

It is not surprising that this analysis indicates such a difference in these estimates, considering the large number of variables that have been ignored. However, this analysis provides an idea of the probable magnitude of the meander migration. It can also be used with additional analysis to assess if bank protection is necessary.

654.1206 Conclusion

In the natural system, there are rarely perfectly linear or straight systems. Natural systems that appear linear typically have some slight sinuosity to them.

Natural channel work requires that the proposed design fits into the natural system within the physical constraints imposed by other project objectives and riparian conditions. Design requires not only channel planform design but also an assessment of natural variability, as well as potential channel movement.

Planform design parameters include sinuosity, meander wavelength, an appropriate channel length for one meander wavelength, and trace of the channel. The approach used to perform this design should be appropriate to the stream conditions. In a threshold channel, planform relates to establishing a maximum slope based on critical stability of the boundary material. In an alluvial channel, planform is a separate dependent variable that must be determined within natural geomorphic limits.

Channel sinuosity is determined from the calculated channel slope and valley slope. To determine other parameters, analogy, hydraulic geometry, and/or analytical methods are employed. To apply the analogy method, a reference reach is located on either the study stream or another suitable stream. From the reference reach a template for the meander planform is developed for the project reach. This may often be problematic due to the nonavailability of a reference reach or subtle, but important fluvial, sedimentary, or morphological differences between it and the study reach.

Alternatively, meander wavelength can be determined using hydraulic geometry techniques. The most reliable hydraulic geometry relationship is wavelength versus width. As with the determination of channel width, preference is given to wavelength predictors from stable reaches of the existing stream either in the project reach or in reference reaches. The channel trace may also be determined analytically using the sine-generated curve. Finally, a string cut to the appropriate length can be laid on a map and fit to existing constraints and to the proper wavelength to form a meandering planform.

The methods used to estimate variability in cross section, as well as potential bank migration, are dependent on site-specific conditions. Some guidance developed for regionally specific studies has been presented. While this material provides a guideline, it should only be used with caution if applied elsewhere.